Analysis of an End Launcher for a Circular Cylindrical Waveguide

M. D. DESHPANDE, MEMBER, IEEE, AND B. N. DAS

Abstract—**The analysis of an end launcher type of transition exciting dominant TE_{11} mode circular waveguide from a coaxial line is presented. The expressions for real and imaginary parts of the input impedance seen by the coaxial line are derived for the general case of offset launcher using self reaction of the assumed current over the loop. The dimensions of combined electric and magnetic loops having low input VSWR are determined. There is satisfactory agreement between theoretical and experimental results.**

I. Introduction

A RADIAL PROBE driven through a coaxial line may be used to excite a dominant TE_{11} mode in a circular cylindrical waveguide [1]. For the excitation of two-dimensional array of closely packed circular waveguides use of a collinear end launcher type of transition (Fig. 1(a)) instead of radial probe has been suggested [2]–[4]. The analysis of such a launcher [4] has been restricted to the case where the longitudinal arm of the rectangular loop is coincident with z-axis of the waveguide ("concentric launcher"). An expression for the resistive part of the input impedance seen by the coaxial line has been derived and used for the design of the transition. The reactance cancellation has been obtained by using a stub collinear with the longitudinal arm of the loop. Since analytical expression for reactive part of the input impedance was not available the length of the stub has been determined by trial and error method. The bandwidth of such a device is extremely narrow. If the expressions for both resistive and reactive parts of the input impedance seen by the coaxial line are known, the bandwidth of the device can be exactly determined and a method of its improvement can be found.

In the present paper expressions for both real and imaginary parts of the input impedance, seen by a coaxial line exciting through a rectangular loop (Fig. 1(a)) a dominant TE_{11} mode circular waveguide are derived from the self reaction of assumed currents in the longitudinal and radial arms of the loop. The analysis is applicable not only to a concentric launcher but also to a launcher with longitudinal arm of the loop not coincident with z-axis of the waveguide ("offset launcher"). Analysis is carried out by assuming that the radial arm of the loop is replaced by a curvilinear metallic strip in the cross section of the waveguide [1]. For the calculation of self reaction the expressions for electric field in the waveguide due to currents in radial and longitudinal arms of the loop are separately determined following the methods suggested in the literature [5], [6]. Expressions for the parameters of the equivalent network of the junction between coaxial and circular waveguide terminated into a matched load are, then, obtained in terms of lengths L_1 and l of the longitudinal and radial arms of the loop.

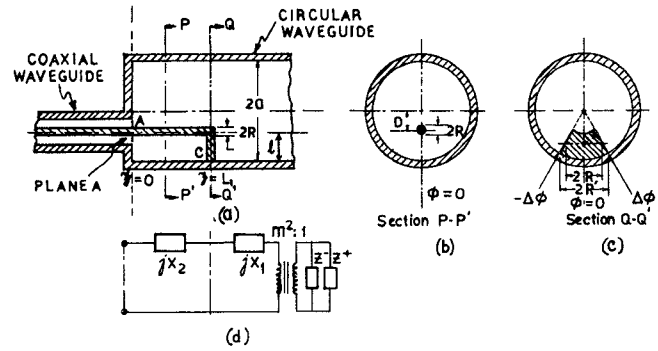

Fig. 1. An offset end launcher for a circular waveguide terminated into matched load. (a) Longitudinal sectional view, *ABC*-rectangular loop, *AB*-longitudinal arm, *BC*-radial arm. (b) Transverse section view at plane *PP'*. (c) Transverse sectional view at plane *QQ'*. (d) Equivalent circuit.

The resistive part of the input impedance is evaluated for $0.6 \leqslant l \leqslant 0.8$-cm (offset launcher) and also for $l = 1.15$-cm (concentric launcher), and L_1 in the range $0.9 \leqslant L_1 \leqslant 1.5$ cm. The variation of input reactance with frequency is, then, computed for combinations of L_1 and l which gives the resistive part of the input impedance close to 50 Ω. From variation of input impedance as a function of frequency the dimensions L_1 and l of the loop which give low VSWR over a range of frequencies are determined. A comparison between theoretical and experimental results on input VSWR for an offset launcher with $L_1 = 1.4$ cm, $l = 0.7$ cm, $a = 1.15$ cm, and $R = 0.15$ cm is presented.

II. Analysis

Fig. 1(a) shows a coaxial line exciting a dominant TE_{11} mode circular waveguide through an end launcher. The input impedance seen by the coaxial line at the reference

Manuscript received November 7, 1977; revised March 13, 1978.

The authors are with the Department of Electronics and Electrical Communication Engineering, Indian Institute of Technology, Kharagpur 721302, India.

0018-9480/78/0900-0672$00.75 ©1978 IEEE

point A is given by the stationary formula [5]

$$Z_{\text{in}}|_A = -\frac{\int_v \vec{E}_{AB}\cdot\vec{J}_{AB}\,dv}{I_{\text{in}}^2} - \frac{\int_v \vec{E}_{BC}\cdot\vec{J}_{BC}}{I_{\text{in}}^2} \tag{1}$$

where $\vec{E}_{AB}$ and $\vec{E}_{BC}$ are the electric fields inside the waveguide due to currents $\vec{J}_{AB}=\vec{U}_z j_{AB}$, and $\vec{J}_{BC}=\vec{U}_\rho j_{BC}$ in the longitudinal and radial arms, respectively, of the loop ABC and I_{in} is the input current at reference point A. The electric field E_{ABz} is related to z-directed vector potential A_z through the equation.

$$E_{ABz} = \frac{1}{j\omega\epsilon}\left[\frac{\partial^2 A_z}{\partial z^2} + K^2 A_z\right] \tag{2}$$

where A_z is given by [6]

$$A_z = \int_v dv \sum_{n=0}^{\infty}\sum_{p=1}^{\infty} \frac{\epsilon_n}{2\pi a^2 \nu} j_{AB}(\rho',\phi',z') \cdot \frac{J_n(x_p\rho')J_n(x_p\rho)}{\left[J_n'(x_p a)\right]^2}\cos(n\phi)e^{\pm\nu(z-z')}. \tag{3}$$

In (3) $\epsilon_n=1$ for $n=0$ and $\epsilon_n=2$ for $n\neq 0$, $x_p a$ is the pth root of $J_n(x)=0$, $\nu=\sqrt{x_p^2-K^2}$, + and − signs in the exponential correspond to $z-z'<0$ and $z-z'>0$ regions, respectively. The primed variables, ρ',ϕ',z' and unprimed variables ρ,ϕ,z correspond to source and field points, respectively. For the filametary current (as shown in Fig. 1(b)) the volume integrals appearing in (3) and in the first term of right-hand side of (1) reduce to line integrals. Considering the effect of conducting plate at $z=0$ plane, the expression for potential A_z due to current in the longitudinal arm of the loop becomes

$$A_z(\rho,\phi,z) = \int_{-L_1}^{L_1}\sum_{n=0}^{\infty}\sum_{p=1}^{\infty} \frac{\epsilon_n}{2\pi a^2\nu} j_{AB}(D,0,z') \cdot \frac{J_n(x_p D)J_n(x_p\rho)}{\left[J_n'(x_p a)\right]^2}\cos(n\phi)e^{\pm\nu(z-z')}dz'. \tag{4}$$

For convenience in the analysis the radial arm of the loop is assumed to be replaced by a curvilinear metallic strip (as shown in Fig. 1(c)) in the cross-sectional plane $z=L_1$. The volume integral in the second term of right-hand side of (1) reduces to surface integral. The transverse component E_{BCt} of electric field $\vec{E}_{BC}$ at $z=L_1$ due to current J_{BC} in the radial arm is of the form [5]

$$\vec{E}_{Bct} = \sum_{i=0}^{\infty} \frac{Z_i\left(-\int\int_{\text{surface}} \vec{e}_i\cdot\vec{J}_{BC}\,ds\right)\vec{e}_i}{(1-\Gamma_i^-)/(1+\Gamma_i^-)+(1-\Gamma_i^+)/(1+\Gamma_i^+)} \tag{5}$$

where $\vec{e}_i$ is the normalized vector mode function, Γ_i^+ and Γ_i^- are, respectively, $+z$ and $-z$ reflection coefficients for ith mode at reference plane $z=L_1$ and Z_i is the modal admittance. Using (2)–(5) the expression for input impedance is obtained as

$$Z_{\text{in}}|_A = -\frac{\int_0^{L_1} E_{ABz} j_{AB}(D,0,z')dz'}{I_{\text{in}}^2} + \frac{1}{I_{\text{in}}^2}\sum_{i=0}^{\infty}\frac{Z_i\left(\int\int_{\text{surface}}\vec{e}_i\cdot\vec{J}_{BC}\,ds\right)^2}{(1-\Gamma_i^-)/(1+\Gamma_i^-)+(1-\Gamma_i^+)/(1+\Gamma_i^+)}. \tag{6}$$

The circular waveguide supports only dominant ($i=0$) TE_{11} mode. The current $\vec{J}_{AB}$ excites only TM modes (TM_{0p} for $D=0$ and TM_{np} for $D\neq 0$) which are higher order modes in the waveguide. Further Z_i is real for $i=0$, imaginary for $i\neq 0$ and $\Gamma_i^{\pm}=0$ for $i\neq 0$. Equation (6) can, therefore, be written as [1], [5]

$$Z_{\text{in}}|_A = jX_\rho + jX_i + m^2 Z^+ Z^-/(Z^+ + Z^-) \tag{7}$$

where

$$X_2 = -\frac{1}{I_{\text{in}}^2}\int_0^{L_1} E_{ABz} j_{AB}\,dz' \tag{7a}$$

and the junction between coaxial and circular waveguide may be represented by the equivalent network of Fig. 1(d). The parameters of equivalent circuit can be determined from a knowledge of current distributions $\vec{J}_{AB}$ and $\vec{J}_{BC}$ over the longitudinal and radial arms respectively of the loop ABC (Fig. 1). These current distributions are found to be of the form [4]

$$\vec{J}_{AB} = \vec{U}_z\frac{I_0}{2\pi R}\cos K(L_1+l-z'), \quad \text{for } \rho'=D,\ \phi'=0$$
$$=0, \quad \text{elsewhere} \tag{8}$$

and

$$\vec{J}_{BC} = \vec{U}_\rho\frac{I_0}{2R}\cos K(a-\rho'), \quad \text{for } -\Delta\phi\leqslant\phi\leqslant\Delta\phi$$
$$=0, \quad \text{elsewhere} \tag{9}$$

where

$$\Delta\phi = R'/a \approx R/a.$$

In view of the stationary character of the expression for input impedance, it is assumed that the radius R of the thin cylindrical conductor is approximately equal to average between maximum and minimum widths of the curvilinear metallic strip.

III. Expression for the Parameters of Equivalent Network and Input VSWR

From (2), (4), and (8) the expression for the axial component, $E_{ABz}(\rho,\phi,z)$ of the electric field in the region $z>0$ is obtained as

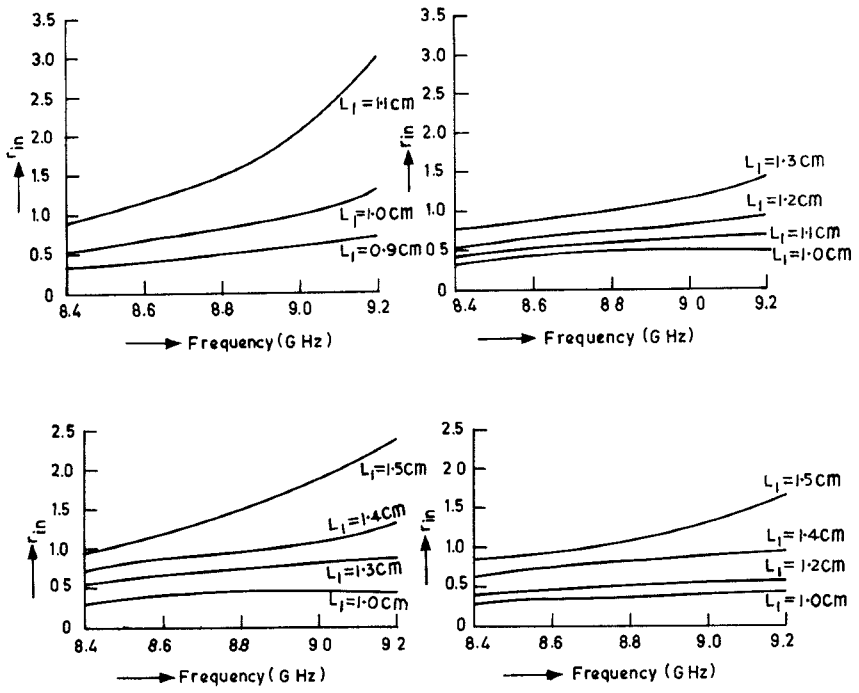

Fig. 2. Variation of real part of the normalized input impedance versus frequency. (a) $l=1.15$ cm (concentric launcher). (b) $l=0.8$ cm. (c) $l=0.7$ cm. (d) $l=0.6$ cm.

$$E_{ABz}(\rho,\phi,z)=\frac{1}{j\omega\epsilon}\sum_{n=0}^{\infty}\sum_{p=1}^{\infty}\frac{I_0}{\pi a^2 v}\frac{J_n(x_pD)J_n(x_p\rho)}{[J_n'(x_pa)]^2}\cos(n\phi)$$
$$\{K\bar{e}^{vz}\sin K(L_1+l)-\bar{e}^{vL_1}\cosh(vz)\cdot[v\cos(Kl)-K\sin(Kl)]\}. \quad (10)$$

Substituting (10) and (8) into (7a), and after performing the integration, the expression for X_2 is obtained in the form:

$$X_2=\frac{120}{\cos^2K(L_1+l)}\sum_{n=0}^{\infty}\sum_{p=1}^{\infty}\left[\frac{J_n(x_pD)}{J_n'(x_pa)}\right]^2\frac{1}{(x_pa)^2}$$
$$\cdot\Big[\sin^2K(L_1+l)+\sin 2K(L_1+l)-2\bar{e}^{vL_1}\sin K(L_1+l)$$
$$\cdot\left\{\cos(Kl)+\frac{K}{v}\sin(Kl)\right\}+\left(\frac{K}{v}\sin Kl\right)^2-\cos^2(Kl)+\bar{e}^{2vL_1}$$
$$\cdot\left\{\frac{K}{v}\sin(Kl)+\cos(Kl)\right\}^2\Big]. \quad (11)$$

Using expressions for normalized vector mode functions available in the literature [1] and (6)–(9), the parameters m^2 and X_1 of the equivalent network of Fig. 1(d) are obtained in the form:

$$m^2=\frac{2}{\pi(x_{11}^{12}-1)}\frac{1}{J_1^2(x_{11}^1)}\left[\frac{\sin(R/a)}{R/a}\right]^2$$
$$\cdot\frac{1}{\cos^2K(L_1+l)}\left[\int_{1-l/a}^{1}\cos(Ka(1-x))J_1(x_{11}^1x)dx\right]^2 \quad (12)$$

$$X_1=-\sum_{n=0}^{\infty}\sum_{p=1}^{\infty}\frac{60\epsilon_n}{J_{n+1}^2(x_{np})}\frac{\sqrt{(x_{np}/ka)^2-1}}{\cos^2(K(L_1+l))}\left[\frac{\sin(nR/a)}{nR/a}\right]^2$$
$$\cdot\left[\int_{1-l/a}^{1}\cos(Ka(1-x))J_n(x_{np}x)x\,dn\right]^2. \quad (13)$$

From (7) the expressions for real and imaginary parts of the input impedance normalized with respect to characteristic impedance Z_{0c} (50 Ω) of the coaxial line are obtained as

$$\gamma_{in}=\frac{m^2Z_0}{Z_{0c}}\tan^2(\beta_0L_1)/(1+\tan^2(\beta_0L_1)) \quad (14)$$

$$jx_{in}=j(X_1+X_2+X_3)/Z_{0c} \quad (15)$$

where

$$X_3=m^2Z_0\tan(\beta_0L_1)/(1+\tan^2(\beta_0L_1). \quad (16)$$

The magnitude of reflection coefficient at the reference point A, is then

$$|r|=\frac{\sqrt{[(\gamma_{in}-1)^2+x_{in}^2]}}{\sqrt{[(\gamma_{in}+1)^2+x_{in}^2]}} \quad (17)$$

and VSWR in the coaxial line is given by

$$\text{VSWR}=\frac{1+|r|}{1-|r|}.$$

IV. Results

The variation of real part of the normalized input impedance seen by the coaxial line is computed from expression (14) is presented in Fig. 2 for $a=1.15$ cm,

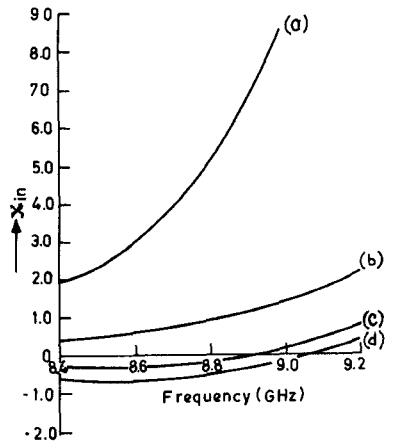

Fig. 3. Variation of imaginary part of the normalized input impedance versus frequency. Curve *a*: $l=1.15$ cm, $L_1=1.0$ cm; curve *b*: $l=0.8$ cm, $L_1=1.3$ cm; curve *c*: $l=0.7$ cm, $L_1=1.4$ cm; curve *d*: $l=0.6$ cm, $L_1=1.5$ cm.

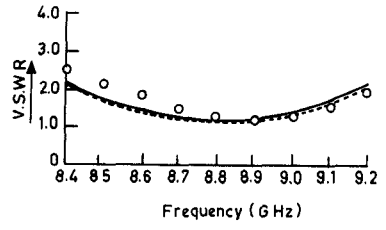

Fig. 4. Variation of input VSWR versus frequency. —— for $l=0.7$ cm, $L_1=1.4$ cm; ---- for $l=0.6$ cm, $L_1=1.5$ cm; o·o·o. Experimental points for $l=0.7$ cm, $L_1=1.4$ cm.

$R=0.15$ cm, $0.6\leqslant l\leqslant 0.8$ cm (offset launcher), $l=1.15$ (concentric launcher), and L_1 in the range $0.9\leqslant L_1\leqslant 1.5$ cm. It is found from Fig. 2 that the curve for variation of the real part of the input impedance crosses the 50-Ω line for the cases ($L_1=1.0$ cm, $l=1.15$ cm), ($L_1=1.3$ cm, $l=0.8$ cm), ($L_1=1.4$ cm, $l=0.7$ cm), and ($L_1=1.5$ cm, $l=0.6$ cm).

The expressions (11) and (13) for X_2 and X_1 are in the form of double infinite series for the offset launcher. It is found that the terms $p=1$, $n=0,1,\cdots 12$ have significant contribution to X_1 and contribution of other terms is negligibly small. For infinite series (11) contribution of the terms other than $n=0,1,2\cdots 7$ and $p=1,2,\cdots 5$ is negligible. For the case of concentric launcher ($l=1.15$ cm) the double summation in (11) reduces to single summation ($n=0$ and $p=1,2\cdots 12$). The variation of the total input reactance, x_{in} with frequency is evaluated from (15), (16), (13), and (11), and is presented in Fig. 3 for above four cases. The results of Fig. 2 and Fig. 3 are used to evaluate input VSWR from (18). The input VSWR is greater than 2.0 for ($L_1=1.0$ cm, $l=1.15$ cm) and ($L_1=1.3$ cm, $l=0.8$ cm), and is quite low for the other two cases. The variation of input VSWR for the cases ($L_1=1.4$ cm and $l=0.7$ cm) and ($L_1=1.5$ cm, $l=0.6$ cm) is presented in Fig. 4. An offset launcher is fabricated for $L_1=1.4$ cm, $l=0.7$ cm. The experimental results on input VSWR are also presented in Fig. 4.

V. Conclusion

The self reaction concept has been used to obtain a network representation of end launcher exciting a dominant TE_{11} mode circular waveguide from a coaxial line. There is a good agreement between theoretical and experimental results on input VSWR in the frequency range 8.5 to 9.2 GHz. In this frequency range minimum VSWR attained theoretically and experimentally is of the order of 1.2. The frequency at which the input reactance is zero and that at which the input resistance is 50 Ω are functions of L_1 and l. These two frequencies are found to be different. Further reduction in input VSWR is possible through an adjustment of L_1 and l such that the difference between two frequencies is reduced.

The results of analysis show that for the particular range of L_1 and l chosen, the concentric launcher has a very high input reactance and cannot, therefore, be used without a stub for reactance cancellation. Using a collinear stub reactance cancellation is obtained over an extremely narrow frequency range [4]. An offset launcher without any additional arrangement for reactance cancellation has low input VSWR over a relatively wider frequency range. This can be attributed to the fact that as the launcher is displaced from the axis of the waveguide the amplitudes of significant higher order modes decrease. The resulting decrease in the energy storage reduces the input reactance.

Acknowledgment

The authors thank Prof. G. S. Sanyal and Prof. J. Das for their kind interest in the work.

References

[1] M. D. Deshpande and B. N. Das, "Input impedance of coaxial line to circular waveguide feed," *IEEE Trans. Microwave Theory Tech.*, vol. MTT-25, pp. 954–957, Nov. 1977.

[2] J. Cershon and R. Wheeler, "Broad band waveguide to coaxial transition," *IRE Convention Record* Pt. 1, 1957, pp. 182–190.

[3] R. Tang and N. S. Wong, "Multimode phased array element for wide scan angle impedance matching," *Proc. IEEE*, vol. 56, Nov. 1968, pp. 1951–1959.

[4] B. N. Das and G. S. Sanyal, "Coaxial to waveguide transition (end launcher type)," *Proc. Inst. Elec. Eng.*, vol. 123, no. 10, Oct. 1976, pp. 984–986.

[5] R. F. Harrington, *Time Harmonic Electromagnetic Field.* New York: McGraw-Hill 1961, ch. 8, pp. 381–440.

[6] G. Markov, *Antennas.* Moscow: Progress Publishers, ch. 7, pp. 207–211.